

# Study of the $^{26}\text{Al}^m(d,p)^{27}\text{Al}$ reaction and the influence of the $^{26}\text{Al} 0^+$ isomer on the destruction of $^{26}\text{Al}$ in the Galaxy

S. Almaraz-Calderon,<sup>1,\*</sup> K. E. Rehm,<sup>2</sup> N. Gerken,<sup>1</sup> M. L. Avila,<sup>2</sup> B. P. Kay,<sup>2</sup> R. Talwar,<sup>2</sup> A. D. Ayangeakaa,<sup>2</sup> S. Bottoni,<sup>2</sup> A. A. Chen,<sup>3</sup> C. M. Deibel,<sup>4</sup> C. Dickerson,<sup>2</sup> K. Hanselman,<sup>1</sup> C. R. Hoffman,<sup>2</sup> C. L. Jiang,<sup>2</sup> S. A. Kuvin,<sup>5</sup> O. Nusair,<sup>2</sup> R. C. Pardo,<sup>2</sup> D. Santiago-Gonzalez,<sup>4,2</sup> J. Sethi,<sup>2</sup> and C. Ugalde<sup>2</sup>

<sup>1</sup>*Department of Physics, Florida State University, Tallahassee, FL 32306, USA*

<sup>2</sup>*Physics Division, Argonne National Laboratory, Argonne, IL 60439, USA*

<sup>3</sup>*Department of Physics and Astronomy, McMaster University, Hamilton ON L8S 4M1, Canada*

<sup>4</sup>*Department of Physics and Astronomy, Louisiana State University, Baton Rouge, LA 70803, USA*

<sup>5</sup>*Department of Physics, University of Connecticut, Storrs, CT 06269, USA*

(Dated: April 11, 2017)

The existence of  $^{26}\text{Al}$  ( $t_{1/2} = 7.17 \times 10^5$  yr) in interstellar medium provides a direct confirmation of ongoing nucleosynthesis in the Galaxy. The presence of a low-lying  $0^+$  isomer ( $^{26}\text{Al}^m$ ), however, severely complicates the astrophysical calculations. We present for the first time a study of the  $^{26}\text{Al}^m(d,p)^{27}\text{Al}$  reaction using an isomeric  $^{26}\text{Al}$  beam. The selectivity of this reaction allowed the study of  $\ell = 0$  transfers to  $T = 1/2$ , and  $T = 3/2$  states in  $^{27}\text{Al}$ . Mirror symmetry arguments were then used to constrain the  $^{26}\text{Al}^m(p,\gamma)^{27}\text{Si}$  reaction rate and provide an experimentally determined upper limit of the rate for the destruction of isomeric  $^{26}\text{Al}$  via radiative proton capture reactions, which is expected to dominate the destruction path of  $^{26}\text{Al}^m$  in Asymptotic Giant Branch stars, Classical Novae and Core Collapse Supernovae.

PACS numbers: 25.60.-t, 25.60.Je, 26.20.Np, 26.50.+x

The detection of the characteristic 1.809-MeV  $\gamma$ -ray line from the decay of the long-lived radioisotope  $^{26}\text{Al}$  ( $t_{1/2} = 7.17 \times 10^5$  yr) in the interstellar medium by  $\gamma$ -ray satellites [1, 2] has demonstrated that nucleosynthesis is an ongoing process in the Galaxy, confirming earlier measurements of excess  $^{26}\text{Mg}$  in meteorites [3–5] and presolar dust grains [6, 7]. The COMPTEL and INTEGRAL satellite missions have produced detailed maps of the  $^{26}\text{Al}$  distribution across the Galaxy [2, 8, 9]. From the observed  $\gamma$ -ray intensity an equilibrium mass of  $\sim 2$ –3 solar masses of  $^{26}\text{Al}$  in the entire Galaxy [8] has been inferred. Moreover, the observed distribution of 1.809 MeV  $\gamma$ -rays points to massive stars as the main production sites of  $^{26}\text{Al}$  [2, 10, 11]. A number of different sources of  $^{26}\text{Al}$  have been suggested. It is expected that Galactic  $^{26}\text{Al}$  is produced predominately in massive Wolf-Rayet (WR) stars either during the hydrogen-burning phase or their core collapse supernova (CCSN) phase [8], with additional contribution from asymptotic giant branch (AGB) stars and classical novae (CN) [12, 13]. The existence of a short-lived ( $t_{1/2} = 6.4$  s) isomeric state, located 228 keV above the ground state, severely complicates the calibration of its nucleosynthesis [14]. While transitions between the isomeric state ( $^{26}\text{Al}^m$ ,  $J^\pi = 0^+$ ) and the ground state ( $^{26}\text{Al}^g$ ,  $J^\pi = 5^+$ ) are strongly inhibited by the large spin difference ( $\Delta J = 5$ ), they may communicate with each other via thermal excitations involving higher-lying levels in  $^{26}\text{Al}$  [15] which puts constraints on the production and destruction processes of  $^{26}\text{Al}$  in astrophysical environments.

In AGB stars, CN and CCSN the destruction of  $^{26}\text{Al}$  is governed by radiative proton capture reactions on  $^{26}\text{Al}^g$

and  $^{26}\text{Al}^m$  [14]. The  $^{26}\text{Al}^g(p,\gamma)^{27}\text{Si}$  reaction has been the subject of several studies (e.g. Refs. [16–24]). Among them, a  $\gamma$ -ray spectroscopy study of the  $^{26}\text{Al}^g + p$  resonances in  $^{27}\text{Si}$  was performed where the authors identified low-lying resonances with  $\ell_p = 0$  and  $\ell_p = 2$  captures which strongly influence the rate of the  $^{26}\text{Al}^g(p,\gamma)^{27}\text{Si}$  reaction [20]. The same group also identified  $T = 1/2$  analog states in the  $A = 27$  mirror system [21].

Two recent experiments of the  $^{26}\text{Al}^g(d,p)^{27}\text{Al}$  reaction were conducted to extract spectroscopic information of key resonances in the mirror nucleus  $^{27}\text{Si}$ . From these results the  $^{26}\text{Al}^g(p,\gamma)^{27}\text{Si}$  reaction rate in WR stars and AGB stars is well constrained [23, 24]. For the isomeric state, however, very scarce experimental information is available on the rate of the  $^{26}\text{Al}^m(p,\gamma)^{27}\text{Si}$  reaction [25, 26]. While the results of Ref. [25] provide excitation energies and proton-decay branching ratios for high-lying states in  $^{27}\text{Si}$  ( $E_r^m \geq 445$  KeV), it is also pointed out that the reaction rate could be dominated by unobserved resonances at lower excitation energies. The gamma-ray study of Ref. [26] provided the exact energies of the critical  $\ell = 2$  ( $E_r^m = 146$  keV) and  $\ell = 1$  ( $E_r^m = 378$  keV) states that are expected to dominate the rate in a wide range of temperatures. Sensitivity studies have highlighted uncertainties in this reaction as being of high importance to understand the  $^{26}\text{Al}$  production in massive stars and the isotopic abundances of  $^{26}\text{Mg}$  synthesized in novae environments [14, 27]. In the most recent of such studies, Iliadis *et al.* [14] adopted the ground state rate for the isomeric rate due to the lack of experimental information.

Estimates of the  $^{26}\text{Al}^m(p,\gamma)^{27}\text{Si}$  reaction rate are

presently based on Hauser-Feshbach calculations by scaling the ground state ( $p, \gamma$ ) rate [14, 28–30]. This approximation is inadequate since very different states and configurations are populated by the  $^{26}\text{Al}^g + p$  and  $^{26}\text{Al}^m + p$  proton resonances in  $^{27}\text{Si}$  as has been shown in the study of Deibel *et al.* [25].

Several attempts have been made at different laboratories worldwide to produce an isomeric  $^{26}\text{Al}^m$  beam with sufficient intensity, purity, energy resolution and a high isomer-to-ground-state ratio in order to study nuclear reactions induced by the  $0^+$  isomer in  $^{26}\text{Al}$  [31–34]. This letter reports the measurement of the  $^{26}\text{Al}^m(d, p)^{27}\text{Al}$  reaction using a  $^{26}\text{Al}$  beam with 70% isomeric content. Spectroscopic information of states in  $^{27}\text{Al}$  populated by single-neutron transfers on the  $0^+$ ,  $T = 1$  isomer was extracted. Symmetry considerations between members of the  $A = 27$  mirror system ( $^{27}\text{Al}$ ,  $^{27}\text{Si}$ ) were then used to constrain the  $^{26}\text{Al}^m(p, \gamma)^{27}\text{Si}$  reaction rate in relevant astrophysical scenarios.

The experiment was performed at the ATLAS accelerator facility at Argonne National Laboratory. A 4.6 MeV/u  $^{26}\text{Al}^m$  beam was produced in-flight [35] via the  $^{26}\text{Mg}(p, n)^{26}\text{Al}$  reaction in inverse kinematics. A 6.1 MeV/u primary beam of  $^{26}\text{Mg}$  was used to bombard a gas cell filled with 1 atm of hydrogen gas. The energy of the primary beam and the target pressure in the gas cell were chosen to maximize the production of the isomeric state over the ground state [36, 37]. After the production gas cell, a rebuncher and a  $22^\circ$  bending magnet were used to separate the  $^{26}\text{Al}^{13+}$  beam from the  $^{26}\text{Mg}$  production beam using its different magnetic rigidity. Furthermore, a 12 MHz radio-frequency (RF) sweeper was used to improve the purity of the  $^{26}\text{Al}$  beam [38].

Considerable effort went into confirming the presence and characteristics of the  $^{26}\text{Al}^m$  beam since the presence of a  $^{26}\text{Al}^g$  component will influence the  $(d, p)$  spectrum. In a first step, a test experiment was performed using a rotating stopper setup to measure the purity and isomer content of the beam. The radioactive  $^{26}\text{Al}$  beam was stopped in a 100 mg/cm<sup>2</sup> thick Au-catcher foil mounted at the bottom of a rotating wheel. After an implantation time of 15 sec the foil was rotated by  $180^\circ$  and placed in between two face-to-face NaI detectors where the two coincident 511-keV photons from the  $\beta^+$  decay of  $^{26}\text{Al}^m$  were detected. The measured half-life of  $6 \pm 1$  s confirmed correct identification of  $^{26}\text{Al}^m$ . GEANT4 simulations were performed to calculate the detection efficiencies of the NaI detectors [39]. The coincidence rate was then used to measure the isomer content of the beam using the GEANT4 calculated efficiencies. During the  $\gamma$ -ray counting time of 15 sec the full  $^{26}\text{Al}$  beam ( $^{26}\text{Al}^g + ^{26}\text{Al}^m$ ) was transmitted to the Split-Pole Spectrograph or a silicon detector placed at  $0^\circ$  where the beam was identified with respect to mass, Z and its total energy.

The purity of the  $^{26}\text{Al}$  beam was better than 98% as shown in Fig. 1(a) in a spectrum measured with a silicon

surface barrier detector at  $0^\circ$ . The energy uncertainty of the secondary  $^{26}\text{Al}$  beam was less than 1.2 MeV ( $\sim 1\%$ ). The main contaminant of the  $^{26}\text{Al}^{13+}$  beam came from the primary  $^{26}\text{Mg}^{11+}$  production beam with an energy of 86 MeV while the  $^{26}\text{Mg}^{12+}$  charge state was completely eliminated by the RF sweeper. Fig. 1(b) shows the coincident 511-keV annihilation radiation measured with two NaI detectors. The inset confirms the presence of  $^{26}\text{Al}^m$  through its known 6.35 s half-life. From this beam development run it was established that, for this specific production energy and target thickness,  $70 \pm 10\%$  of the radioactive  $^{26}\text{Al}$  beam was in the isomeric  $0^+$  state.

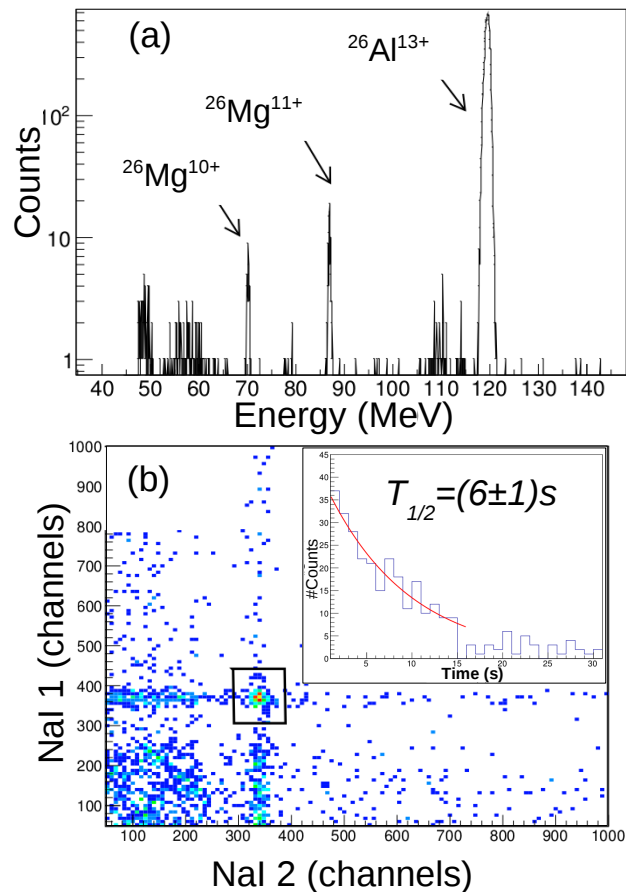


FIG. 1. (color online). Beam characterization. (a) Spectrum of the  $^{26}\text{Al}$  beam measured at  $0^\circ$  in a silicon detector. The main contaminant of the beam is a lower ( $11^+$ ) charge state of the primary  $^{26}\text{Mg}$  production beam. (b) Coincidence spectrum measured with the NaI detectors. The inset in the top right corner shows the half-life of the beam as determined by the 511-keV coincidences which confirms the presence of the isomer.

The  $^{26}\text{Al}(d, p)^{27}\text{Al}$  reaction was measured using a 450  $\mu\text{g}/\text{cm}^2$  thick  $\text{CD}_2$  target which was bombarded by a 120 MeV  $^{26}\text{Al}$  beam with a typical intensity of  $2.5 \times 10^5$  pps. Taking the energy loss into account the energy in the middle of the  $\text{CD}_2$  target was about 117 MeV, very close

to the energy used in the measurement of Ref. [23] using a  $^{26}\text{Al}^g$  beam produced from the negative ion source of the tandem accelerator at ORNL. Two Micron-S1 silicon detectors [40] were placed 45 mm and 90 mm upstream of the target covering an angular range in the laboratory frame of  $133^\circ - 151^\circ$  and  $152^\circ - 165^\circ$ , respectively. Due to the closer geometry and the thicker target compared to the one used in Refs. [23, 24], the energy resolution achieved in this experiment was limited to 120 keV (FWHM). The purity of the beam and its isomeric content were constantly monitored using a ‘characterization’ chamber located  $\sim 1$  m downstream from the reaction target. It consisted of a silicon detector with a  $\times 100$  attenuator and a NaI detector next to a gold catcher foil for a measurement of the annihilation radiation. When the attenuator was in place, the silicon detector was rotated to  $0^\circ$  to measure the purity of the  $^{26}\text{Al}$  beam. The  $^{26}\text{Al}^m/^{26}\text{Al}^g$  ratio of the beam was determined from the yield of the 511-keV  $\gamma$ -rays from the  $\beta^+$  decay of  $^{26}\text{Al}^m$  measured with the NaI detector in a sequence of beam-on, beam-off measurements, and the total  $^{26}\text{Al}$  measured in the silicon detector. During the full experiment the isomer-to-ground-state ratio remained constant with fluctuations of less than 10%.

A separate measurement of the  $(d, p)$  reaction with the main beam contaminant, i.e. 86 MeV  $^{26}\text{Mg}^{11+}$ , which has the same magnetic rigidity as the  $^{26}\text{Al}^{13+}$  beam was also performed. Since protons from the 86 MeV  $^{26}\text{Mg}(d, p)^{27}\text{Mg}$  reaction arrived later at the two Si detectors they could be eliminated by using their different time-of-flight. Similar to the experiments in Refs. [23, 24], a run with a pure carbon target was performed which yielded a smooth background that was scaled to a region containing no peaks from the  $^{26}\text{Al}(d, p)^{27}\text{Al}$  reaction and subtracted from the  $\text{CD}_2$  target data.

The energy spectrum of states populated in the present  $^{26}\text{Al}(d, p)^{27}\text{Al}$  experiment with a 70%  $^{26}\text{Al}^m$  and 30%  $^{26}\text{Al}^g$  beam measured in the angular range  $\theta_{c.m.} \sim 6^\circ - 12^\circ$  is shown in Fig. 2(a) in comparison with the results of Ref. [23] using a pure  $^{26}\text{Al}^g$  beam (Fig. 2(b)). The data of Ref. [23] were folded with a Gaussian of width 120 keV, normalized to the strength of the 3.004 MeV  $9/2^+$  state, which is predominantly populated with the  $^{26}\text{Al}^g$  beam and then subtracted from the energy spectrum measured in this experiment. The resulting spectrum representing states populated by the isomeric  $^{26}\text{Al}(0^+)$  beam, is shown in Fig. 2(c). The shape of the peak at  $\sim 10$  MeV is due to a background of low-energy  $\beta^+$  decay events in the silicon detectors. These events merge with the  $E_{ex} \sim 10$  MeV peak at the most forward angles due to the kinematic compression but are well separated at other angles. The states in Fig. 2 are shown as a function of the  $^{27}\text{Al}$  apparent excitation energy which is calculated using the Q-value for the ground state. Therefore, the states populated by the isomer component of the beam appear shifted down in energy.

The most remarkable feature of the energy spectrum measured with the  $^{26}\text{Al}^m$  beam shown in the bottom panel of Fig. 2 is the high selectivity of the  $(d, p)$  reaction. The spectrum is dominated by the  $1/2^+$  states at  $E_{ex} = 0.84, 6.8$  and  $10.2$  MeV in  $^{27}\text{Al}$  [49]. Transfers to other states (e.g. the  $5/2^+$  ground state in  $^{27}\text{Al}$  are weaker by about one order of magnitude).

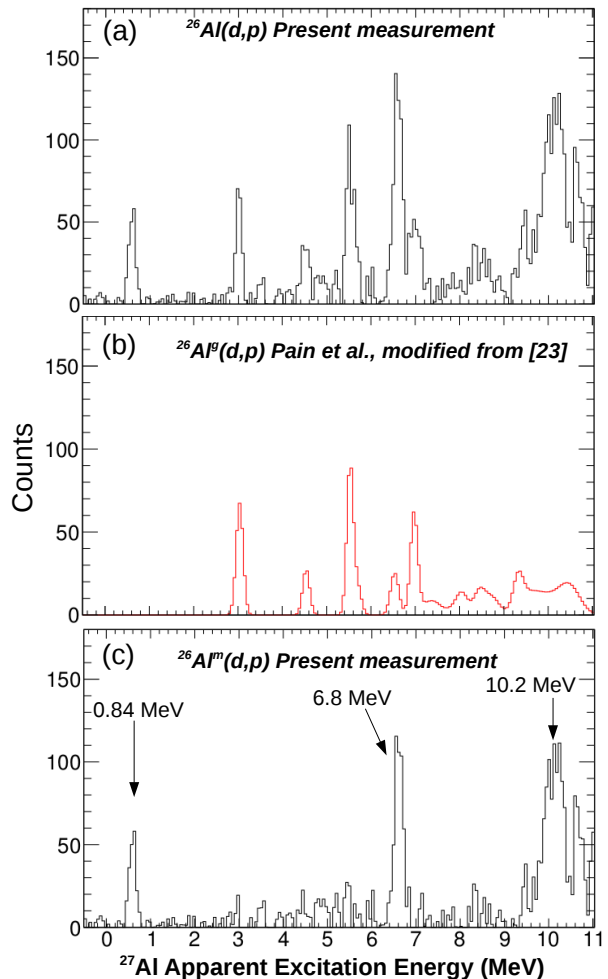


FIG. 2. (color online). (a) Apparent excitation energy spectrum of  $^{27}\text{Al}$  obtained from the  $^{26}\text{Al}(d, p)$  reaction at  $\theta_{c.m.} \sim 6^\circ - 12^\circ$ . A smooth carbon background has been subtracted. The  $^{27}\text{Al}$  excitation energy was calculated using the Q-value for the ground state. Therefore, the states populated by the isomer component of the beam appear shifted down in energy. (b) Data taken from the  $^{26}\text{Al}^g(d, p)$  reaction in a similar angular range [23] folded with a 120 keV Gaussian, normalized to the state at 3.004 MeV are shown for comparison. (c) Apparent excitation energy spectrum of  $^{27}\text{Al}$  obtained from the  $^{26}\text{Al}^m(d, p)$  reaction. The spectrum was obtained by subtracting contributions from the  $^{26}\text{Al}^g$  beam measured in Ref. [23].

The  $9/2^+$  state at 3.004 MeV in  $^{27}\text{Al}$  was used to obtain an absolute beam normalization. This state is dom-

inantly populated via  $\ell = 0$  transfer from the ground state ( $5^+$ ) component of the beam. The angular distribution, shown in Fig.3(a) was fitted with both the adiabatic distorted-wave approximation (ADWA) using the TWOFNR code [41] and the finite-range distorted-wave Born approximation (DWBA) using the PTOLEMY code [42]. In both cases the deuteron bound-state wave function was described using the Argonne  $\nu_{18}$  potential [43], which in the case of ADWA was done using the Johnson-Tandy adiabatic model [44]. The target bound-state form factors were generated using a Woods-Saxon potential with a spin-orbit derivative term, defined by  $r_0 = 1.25$  fm,  $a = 0.65$  fm,  $V_{so} = 6$  MeV,  $r_{so0} = 1.1$  fm, and  $a_{so} = 0.65$  fm. For the DWBA calculations, two sets of global optical-model potentials were explored for the deuterons [45, 46] and similarly for the protons [47, 48]. The same proton potentials were used for the nucleus-nucleon optical potentials in the ADWA calculations. Variations in the resulting spectroscopic factors of less than 10% were seen between the calculated cross sections using the two models and the different combinations of optical-model parameters. The fit to the 3.004 MeV state was normalized so that the spectroscopic factor of 0.49(2) of Ref. [24] was reproduced. This gave us a cross section scale and allowed the total intensity of the  $^{26}\text{Al}^g$  beam to be determined. The total intensity of the  $^{26}\text{Al}^m$  beam was then found using the measured 0.7/0.3 ratio described earlier.

Angular distributions for the three observed transitions to  $1/2^+$  states at  $E_{ex} = 0.84, 6.8$  and  $10.2$  MeV in  $^{27}\text{Al}$  are shown by the solid points in Fig. 3. The distributions are all forward peaked confirming that the  $0^+$  isomeric beam preferentially populates  $2s_{1/2}$  states in  $^{27}\text{Al}$  via  $\ell = 0$  neutron transfers. The solid lines in Fig. 3(b-d) are again DWBA calculations with PTOLEMY assuming an  $\ell = 0$  transfer, populating  $2s_{1/2}$  states in  $^{27}\text{Al}$  at the corresponding excitation energies with their determined spectroscopic factors shown in the insert. The dashed and dotted lines in Fig. 3(b) are examples of angular distributions for  $\ell = 1 - 4$  transfers populating a 0.84 MeV state in  $^{27}\text{Al}$ . These calculations show that  $\ell = 0$  transfer dominate the forward-peaked angular distributions. The uncertainties in Fig. 3 are dominated by the beam normalization and background subtraction. A 15% systematic uncertainty was added in quadrature to the statistical uncertainties to account for these effects.

The populated  $T = 3/2, 2s_{1/2}$  states in our measurement are purely  $\ell = 0$  transfers from the  $^{26}\text{Al}^m$  ( $0^+, T = 1$ ) isomeric beam since  $T = 3/2$  states cannot be reached from the  $^{26}\text{Al}^g$  ( $5^+, T = 0$ ) state. The  $T = 3/2, 2s_{1/2}$  states at  $E_{ex} = 6.81$  MeV and  $E_{ex} = 10.24$  MeV are the strongest peaks in our spectrum. These states are the isobaric analog states of the ground and 3.47 MeV states in  $^{27}\text{Mg}$  [50, 51]. Spectroscopic factors were extracted by fitting the angular distributions with DWBA calculations, giving values of  $C^2S = 0.11(17)$  and  $C^2S = 0.16(24)$ , re-

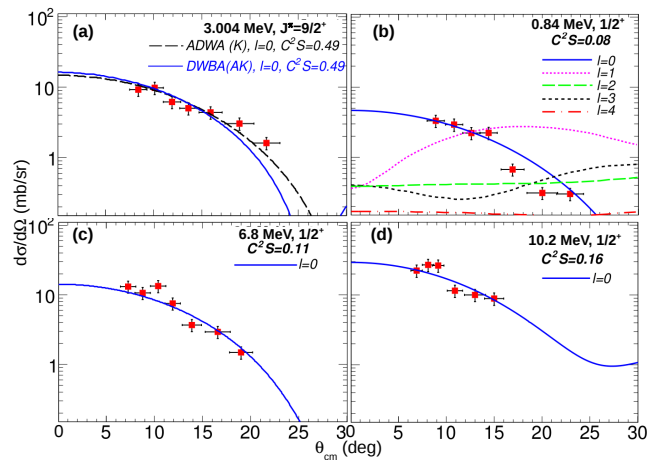


FIG. 3. (color online). (a) Angular distribution and DWBA and ADWA fits for the  $9/2^+$  state in  $^{27}\text{Al}$  at  $E_{ex} = 3.004$  MeV. The data agree with the  $\ell = 0$  transfer from the  $5^+$  ground state component of the beam observed in [24]. A spectroscopic factor,  $C^2S = 0.49$  [24] was used to obtain the absolute beam normalization of the cross section. Angular distributions and DWBA calculations for the states in  $^{27}\text{Al}$  at (b)  $E_{ex} = 0.84$  MeV, (c)  $E_{ex} = 6.8$  MeV, and (d)  $E_{ex} = 10.2$  MeV. These three states are strongly populated by  $\ell = 0$  neutron transfers on the isomeric component of the  $^{26}\text{Al}$  beam.

spectively. In addition, the  $T = 1/2, 1/2^+$  state at 0.84 MeV is also strongly populated in our measurement with an  $\ell = 0$  transfer and a spectroscopic factor of  $C^2S = 0.08(12)$ .

The present highly selective ( $d, p$ ) data allow us to search for states in  $^{27}\text{Al}$  which are mirrors to the states above the proton threshold in  $^{27}\text{Si}$  ( $S_p = 7.463$  MeV) that are expected to dominate the  $^{26}\text{Al}^m(p, \gamma)^{27}\text{Si}$  astrophysical reaction rate. Taking into account an average value for the  $A = 27$  mirror energy differences of  $\sim 200$  keV [21, 52] and a 228 keV energy difference between the ground state and the isomeric state, the states in  $^{27}\text{Al}$  which are mirrors to the astrophysically relevant states in  $^{27}\text{Si}$  are expected between  $E_{ex} \geq 7.9$  MeV and  $E_{ex} \leq 8.5$  MeV. In this energy region the structure of the spectrum measured with the mixed  $^{26}\text{Al}$  beam (Fig.2(a)) is very similar to the one obtained with a pure  $^{26}\text{Al}^g$  (See Fig.2(b)). After subtracting the contribution from the ground state beam, two very small structures remain in our spectra in the astrophysically relevant energy region at  $E_{ex} = 7.9(3)$  MeV and  $E_{ex} = 8.5(3)$  MeV. The yield at  $E_{ex} = 7.9$  MeV agrees with the  $5/2^+$  state reported by Lotay *et al.* [21] at  $E_{ex} = 8.063$  MeV, where this state was assigned to be the mirror of the level at  $E_{ex} = 7.838$  MeV in  $^{27}\text{Si}$  ( $E_r^m = 146$  keV). The yield at  $E_{ex} = 8.5$  MeV could be the mirror of the  $3/2^-$  level at  $E_{ex} = 8.070$  MeV in  $^{27}\text{Si}$  ( $E_r^m = 378$  keV). With the statistics obtained in the present experiment and the experimental energy resolution, no states with spectroscopic factors  $> 0.025$  can

be attributed to transfers from the  $^{26}\text{Al}^m$  beam in this energy region. The 146-keV and 378-keV resonances are expected to dominate the  $^{26}\text{Al}^m(p,\gamma)^{27}\text{Si}$  reaction rate [26]. The same upper limits for the  $^{27}\text{Al}$  spectroscopic factors have also been adopted for the mirror states in  $^{27}\text{Si}$ . Spectroscopic factors of mirror analog states are expected to agree within 20% [24, 53, 54]. For the strength of the 146-keV and 378-keV resonances upper limits of  $0.03 \mu\text{eV}$  and  $165 \text{ meV}$ , respectively have been extracted from this experiment. This allows us to calculate limits of the astrophysical rate of the  $^{26}\text{Al}^m(p,\gamma)^{27}\text{Si}$  reaction which are solely based on experimental data. This rate is shown in Fig. 4(a) in comparison with the recommended NACRE rate of Angulo [29, 30], and the ground state rate extracted from Refs. [20, 23, 24].

For astrophysical temperatures of  $T_9 \text{ (GK)} \leq 0.15$ , typical of AGB stars, the 146-keV resonance dominates the rate. At these temperatures, no significant contribution of the isomeric state to the abundance of  $^{26}\text{Al}$  is expected. However, the reaction rate calculated in this work is important for the accurate determination of the isotopic abundance of  $^{26}\text{Mg}$  synthesized in such environments. For astrophysical temperatures between  $0.2 \leq T_9 \leq 1.0$ , typical of oxygen-neon novae and CCSN, the reaction rate is dominated by the 378-keV resonance. For temperatures in this range ( $T_9 \geq 0.3$ ), the  $^{25}\text{Al}(p,\gamma)^{26}\text{Si}$  reaction competes significantly with the  $\beta$ -decay of  $^{25}\text{Al}$ , leading to a significant abundance of  $^{26}\text{Al}$  in its isomeric state [55]. Moreover, at these temperatures communication between the ground state and the isomeric state is expected through thermal excitations. The ratio between isomeric and g.s. rates is shown in Fig. 4(b). The solid curve gives the ratio based on experimental data presented in this paper and that of Refs. [20, 23, 24] while the dashed curve is based on the recommended NACRE/REACLIB calculations [29, 30, 56]. At temperatures  $T_9 \geq 0.3$  the destruction rates via proton capture in the isomer and ground state are comparable and would need to be properly included in network calculations to account for the observed abundance of  $^{26}\text{Al}$  synthesized in such environments. At temperatures  $T_9 \leq 0.3$  no significant contribution of the isomeric state to the abundance of  $^{26}\text{Al}$  is expected. This behavior is different from the one expected from the NACRE/REACLIB calculations shown by the dashed curve in Fig. 4(b) where the NACRE calculations overestimates the  $^{26}\text{Al}^m(p,\gamma)^{27}\text{Si}$  rate in the temperature range  $T_9 \leq 0.5$ . It was already pointed out by Lotay *et al.* [26], that a Hauser-Feshbach approach is not appropriate where single resonances are expected to dominate the rate.

In summary, we developed and characterized a high-quality  $^{26}\text{Al}$  isomeric beam and used it to perform a study of the  $^{26}\text{Al}^m(d,p)^{27}\text{Al}$  reaction. This highly-selective reaction preferentially populates  $\ell = 0$ ,  $T = 3/2$  and  $T = 1/2$  states in  $^{27}\text{Al}$  providing a powerful spectroscopic tool. Mirror symmetry arguments between  $^{27}\text{Al}$  and  $^{27}\text{Si}$  were

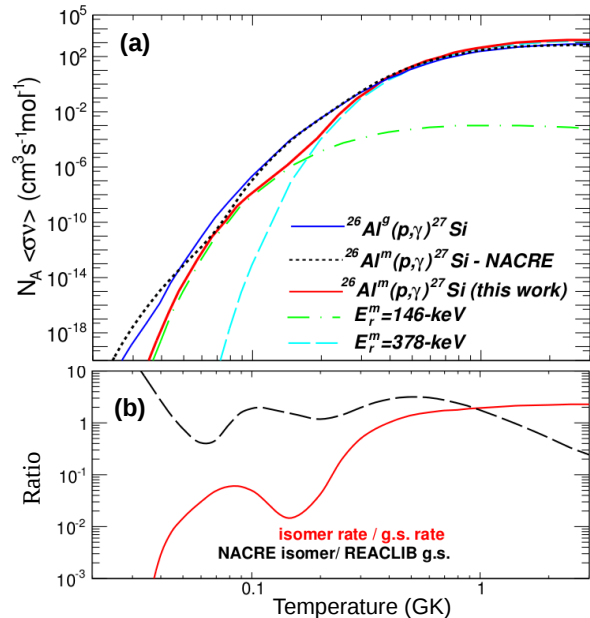


FIG. 4. (color online). (a) Upper limit for the rate of the  $^{26}\text{Al}^m(p,\gamma)^{27}\text{Si}$  reaction in stellar environments as a function of the Temperature. The rate calculated in this work is shown in comparison with the ground state (g.s.) rate, and the recommended NACRE isomeric rate [29, 30]. The g.s. rate was calculated using the parameters of Refs. [20, 23, 24]. (b) Ratios between the isomeric rate calculated in this work and the ground state (solid line) and the corresponding NACRE/REACLIB recommended rates (dashed line) [29, 30, 56].

used to search for astrophysically relevant states to constrain the  $^{26}\text{Al}^m(p,\gamma)^{27}\text{Si}$  reaction rate. This provides, for the first time, with data from previous experimental studies, an upper limit for the reaction rate relevant for the destruction of Galactic  $^{26}\text{Al}$  in AGB stars, CN and CCSN as well as for the accurate determination of isotopic abundances of  $^{26}\text{Mg}$  in such environments.

This work was partially supported by the State of Florida, and the US Department of Energy, Office of Nuclear Physics, under Contracts No. DEAC02-06CH11357 and DE-FG02-96ER40978. This research used resources of ANL's ATLAS facility, which is a DOE Office of Science User Facility.

\* salmarazcalderon@fsu.edu

- [1] W. A. Mahoney, J. C. Ling, A. S. Jacobson, and R. E. Lingenfelter, *Astrophys. J.* **262**, 724 (1982).
- [2] R. Diehl, C. Dupraz, K. Bennett, H. Bloemen, W. Hermsen, J. Knödseder, G. Lichti, D. Morris, J. Ryan, V. Schoenfelder, H. Steinle, A. Strong, B. Swanenburg, M. Varendorff, and C. Winkler, *Astron. Astrophys.* **298**, 445 (1995).

- [3] G.J. MacPherson, A.M. Davis, E.K. Zinner, *Meteoritics* **30**, 365 (1995).
- [4] T. Lee, D. A. Papanastassiou, G. J. Wasserburg, *Astrophys. J.* **211**, L107 (1977).
- [5] J. G. Bradley, J. C. Huneke, G. J. Wasserburg, *J. Geophys. Res.* **83**, 244 (1978).
- [6] P. Hoppe, S. Amari, E. Zinner, T. Ireland, R.S. Lewis, *Astrophys. J.* **430**, 870 (1994).
- [7] G. R. Huss, I. D. Hutcheon, G. J. Wasserburg, *Geochim. Cosmochim. Acta* **61**, 5117 (1997).
- [8] R. Diehl, H. Halloin, K. Kretschmer, G. G. Lichti, V. Schoenfelder, A. W. Strong, A. von Kienlin, W. Wang, P. Jean, J. Knödseder, J.-P. Roques, G. Weidenspointner, S. Schanne, D. H. Hartmann, C. Winkler and C. Wunderer, *Nature*, **439**, 45 (2006).
- [9] W. Wang, M. G. Lang, R. Diehl, H. Halloin, P. Jean, J. Knödseder, K. Kretschmer, P. Martin, J.-P. Roques, A. W. Strong, C. Winkler, X. L. Zhang, *Astron. Astrophys.* **496**, 713 (2009).
- [10] N. Prantzos, and R. Diehl, *Phys. Rep.* **267**, 1 (1996).
- [11] N. Prantzos, *Astrophys. J.* **405**, L55 (1993).
- [12] L. Siess, and M. Arnould *Astron. Astrophys.* **489**, 395 (2008).
- [13] J. Jose, M. Hernanz, and A. Coc, *Astrophys. J.* **479**, L55 (1997).
- [14] C. Iliadis, A. Champagne, A. Chieffi, and M. Limongi, *Astrophys. J. Supp. Ser.* **193**, 16 (2011).
- [15] R. C. Runkle, A. E. Champagne, and J. Engel, *Astrophys. J.* **556**, 970 (2001).
- [16] R. B. Vogelaar, Ph.D. Thesis, California Institute of Technology, 1989, unpublished.
- [17] T.F. Wang, A. E. Champagne, J. D. Hadden, P. V. Magnus, M. S. Smith, A. J. Howard, P. D. Parker, *Nucl. Phys. A* **499**, 546 (1989).
- [18] R. B. Vogelaar, L. W. Mitchell, R. W. Kavanagh, A. E. Champagne, P. V. Magnus, M. S. Smith, A. J. Howard, P. D. Parker, and H. A. OBrien, *Phys. Rev. C* **53**, 1945 (1996).
- [19] C. Ruiz, A. Parikh, J. Jose, L. Buchmann, J. A. Caggiano, A. A. Chen, J. A. Clark, H. Crawford, B. Davids, J. M. DAuria, C. Davis, C. Deibel, L. Erikson, L. Fogarty, D. Frekers, U. Greife, A. Hussein, D. A. Hutcheon, M. Huyse, C. Jewett, A. M. Laird, R. Lewis, P. Mumby-Croft, A. Olin, D. F. Ottewell, C. V. Ouellet, P. Parker, J. Pearson, G. Ruprecht, M. Trinczek, C. Vockenhuber, and C. Wrede, *Phys. Rev. Lett.* **96**, 252501 (2006).
- [20] G. Lotay, P. J. Woods, D. Seweryniak, M. P. Carpenter, R. V. F. Janssens, and S. Zhu, *Phys. Rev. Lett.* **102**, 162502 (2009).
- [21] G. Lotay, P. J. Woods, D. Seweryniak, M. P. Carpenter, H. M. David, R. V. F. Janssens, and S. Zhu, *Phys. Rev. C* **84**, 035802 (2011).
- [22] A. Parikh, K. Wimmer, T. Faestermann, R. Hertenberger, H.-F. Wirth, A. A. Chen, J. A. Clark, C. M. Deibel, C. Herlitzius, R. Kruecken, D. Seiler, K. Setoodehnia, K. Straub, and C. Wrede, *Phys. Rev. C* **84**, 065808 (2011).
- [23] S.D. Pain, D.W. Bardayan, J.C. Blackmon, S.M. Brown, K.Y. Chae, K.A. Chipps, J.A. Cizewski, K.L. Jones, R.L. Kozub, J.F. Liang, C. Matei, M. Matos, B.H. Moazen, C.D. Nesaraja, J. Okoowicz, P.D. OMalley, W.A. Peters, S.T. Pittman, M. Poszajczak, K.T. Schmitt, J.F. Shriner, Jr., D. Shapira, M.S. Smith, D.W. Stracener, and G.L. Wilson, *Phys. Rev. Lett.* **114**, 212501 (2015).
- [24] V. Margerin, G. Lotay, P.J. Woods, M. Aliotta, G. Christian, B. Davids, T. Davinson, D.T. Doherty, J. Fallis, D. Howell, O.S. Kirsebom, D.J. Mountford, A. Rojas, C. Ruiz, and J.A. Tostevin, *Phys. Rev. Lett.* **115**, 062701 (2015).
- [25] C. M. Deibel, J. A. Clark, R. Lewis, A. Parikh, P. D. Parker, and C. Wrede, *Phys. Rev. C* **80**, 035806 (2009).
- [26] G. Lotay, P. J. Woods, D. Seweryniak, M. P. Carpenter, R. V. F. Janssens, and S. Zhu, *Phys. Rev. C* **80**, 055802 (2009). and G. Lotay, P. J. Woods, D. Seweryniak, M. P. Carpenter, R. V. F. Janssens, and S. Zhu, *Phys. Rev. C* **81**, 029903 (2010).
- [27] C. Iliadis, A. Champagne, J. Jose, S. Starrfield, and P. Tupper, *Astrophys. J. Supp. Ser.* **142**, 105 (2002).
- [28] G. R. Caughlan, and W. A. Fowler, *At. Data Nucl. Data Tables* **40**, 283 (1988).
- [29] C. Angulo, M. Arnould, M. Rayet, P. Descouvemont, D. Baye, C. Leclercq-Willain, A. Coc, S. Barhoumi, P. Aguer, C. Rolfs, R. Kunz, J.W. Hammer, A. Mayer, T. Paradellis, S. Kossionides, C. Chronidou, K. Spyrou, S. Degl'Innocenti, G. Fiorentini, B. Ricci, S. Zavatarelli, C. Providencia, H. Wolters, J. Soares, C. Grama, J. Rahighi, A. Shotter, M. Lamehi Racht, *Nucl. Phys. A* **656**, 3 (1999).
- [30] R. H. Cyburt, A. M. Amthor, R. Ferguson, Z. Meisel, K. Smith, S. Warren, A. Heger, R. D. Hoffman, T. Rauscher, A.Sakharuk, H. Schatz, F. K. Thielemann, M. Wiescher *ApJS* **189** 240 (2010).
- [31] TRIUMF proposal 989 (2005).
- [32] O. Grasdjik, BSc. Thesis, KVI (2011), unpublished.
- [33] TAMU Cyclotron Institute Progress Report 2011-2012.
- [34] RIBF-RIKEN proposal NP1512-AVF33 (2015).
- [35] B. Harss, R. C. Pardo, K. E. Rehm, F. Borasi, J. P. Greene, R. V. F. Janssens, C. L. Jiang, J. Nolen, M. Paul, J. P. Schiffer, R. E. Segel, T. F. Wang, P. Wilt, B. Zabransky, *Rev. Sci. Instrum.* **71**, 380 (2000).
- [36] G. Doukellis, J. Rapaport, *Nucl. Phys. A* **467**, 511 (1987).
- [37] R. T. Skelton, R. W. Kavanagh, and D. G. Sargood, *Phys. Rev. C* **35**, 45 (1987).
- [38] R. C. Pardo, J. Bogaty, S. Sharamentov, K.E. Rehm, *Nucl. Inst. Meth. Phys. A* **790**, 1 (2015).
- [39] O. Nusair Ph.D. Thesis, Johann Wolfgang Goethe Universitaet in Frankfurt am Main (2015), unpublished.
- [40] S1-Micron semiconductor.
- [41] J. A. Tostevin, University of Surrey version of the code TWOFNR (of M. Toyama, M. Igarashi, and N. Kishida) and code FRONT (private communication).
- [42] M. H. Macfarlane and S. C. Pieper, ANL-76-11 Rev. 1, Argonne National Laboratory, 1978 (unpublished).
- [43] R. B. Wiringa, V. G. J. Stoks, and R. Schiavilla, *Phys. Rev. C* **51**, 38 (1995).
- [44] R. C. Johnson and P. C. Tandy, *Nucl. Phys. A* **235**, 56 (1974).
- [45] Haixia An and Chonghai Cai, *Phys. Rev. C* **73**, 054605 (2006).
- [46] W. W. Daehnick, J. D. Childs, and Z. Vrcelj, *Phys. Rev. C* **21**, 2253 (1980).
- [47] A. J. Koning and J. P. Delaroche, *Nucl. Phys. A* **713**, 231 (2003).
- [48] R. L. Varner, *Phys. Rep.* **201**, 57 (1991).
- [49] M. S. Basunia, *Nuclear Data Sheets* **112**, 1875 (2011).
- [50] S. Koh and Y. Oda, *Phys. Rev. C* **8**, 2501 (1973).

- [51] R.J. De Meijer, H.F.J. Van Royen, and P.J. Brussaard, Nucl. Phys. A **164**, 11 (1971).
- [52] A.E. Champagne, B.A. Brown, R. Sherr, Nucl. Phys. A **556**, 123 (1993).
- [53] N.K. Timofeyuk, R.C. Johnson, and A.M. Mukhamedzhanov, Phys. Rev. Lett. **91**, 232501 (2003) and N. K. Timofeyuk, R. C. Johnson, and A. M. Mukhamedzhanov, Phys. Rev. Lett. **97**, 069904 (2006).
- [54] N.K. Timofeyui, P. Descouvemont, and R.C. Johnson, Eur. Phys. J. A **27**, 269 (2006).
- [55] P. N. Peplowski, L. T. Baby, I. Wiedenhoefer, S. E. Dekat, E. Diffenderfer, D. L. Gay, O. Grubor-Urosevic, P. Hoefflich, R. A. Kaye, N. Keeley, A. Rojas, and A. Volya, Phys. Rev. C **79**, 032801(R) (2009).
- [56] C. Iliadis, R. Longland, A.E. Champagne, A. Coc, R. Fitzgerald, Nucl. Phys. A **841**, Issues 1-4 (2010).